SAND2017-2180C

10th U. S. National Combustion Meeting
Organized by the Eastern States Section of the Combustion Institute
April 23-26, 2017
College Park, Maryland

Modeling Thermal Runaway in Lithium-ion Packs as a Function of Scale and Heat Source

R. C. Shurtz[1], J. C. Hewson[1,]*

[1]Fire Science and Technology Department
Sandia National Laboratories
PO Box 5800, Albuquerque, NM USA 87185-0836
[*]Corresponding Author Email: jchewso@sandia.gov

Abstract: As deployment of large-scale Li-Ion battery modules is contemplated, there is a need to understand the propensity for thermal runaway in individual cells and the large-scale thermal failure at the pack level. Sources of thermal energy can lead to runaway including short circuits (internal or external), exothermic processes from overcharge of imbalanced cells, the external environment, and other factors. With battery modules consisting of hundreds or even thousands of cells, it will be necessary to design tolerance to local heat release, regardless of the source. This work presents a chemistry-independent framework for analyzing and modeling thermal runaway that will be demonstrated by applying it to thermal runaway (ignition) and cascading failure (propagation).
Keywords: thermal runaway, lithium-ion batteries, ignition, propagation

1. Introduction

As the importance of electrical energy storage increases, the hazards associated with unintentional release of that energy must be addressed. Internally, batteries typically have both fuel and oxidizer, making them a premixed system subject to thermal runaway. Experience with other forms of thermal runaway has led to continually improving best practices, but less experience exists with batteries for large-scale energy storage. Improved understanding of the best approaches is needed to maximize safety through a combination of testing, careful experimentation to understand phenomena and the development of modeling approaches that aid in interpreting and extending measured phenomena. The current industry and regulatory approach to studying battery failures at the system level relies on testing. As system sizes increase there will be requirements to analyze and test increasingly expensive systems. To date, there are no system-level simulation tools that adequately predict the range of processes that occur during thermal runaway in batteries.

Lithium-ion batteries are particularly desirable for energy storage applications because of their high energy and power density. Within lithium-ion batteries a series of exothermic and gas-generating reactions can take place as temperatures rise or as the battery is otherwise put into an unstable state. Some of these reactions are related to the internal battery chemistry while others involve the combustion in air of battery components including hydrocarbon based liquid electrolytes and plastic packaging.

The reactions that are important at the lowest temperatures are those internal to the battery. These include reactions associated with the decomposition of the electrolyte and its reaction with lithium from the anode. At slightly higher temperatures, reactions of the cathode with electrolytes become important. The rate of exothermic reaction at these temperatures is relatively low, and it is possible to consider balances between the heat release and its dissipation leading to an avoidance of thermal runaway.

2. Formulation

In this paper a simplified thermal model is employed. Cells are typically assumed to be nearly homogeneous in temperature with external and inter-cell heat transfer being the limiting process. Masses and heat capacities can be associated with cells and layers of insulting or conducting materials between the cells. Within reactive cells, the evolution of the reactive components will be tracked through their progress variables, Y_i, a normalized mass concentration, that evolve according to the simple homogeneous conservation equation

$$\frac{dY_i}{dt} = -A_i f_i(\mathbf{Y}) \exp\left(-E_i / RT\right) \tag{1}$$

where A_i and E_i are the pre-exponential coefficient and activation energy associated with an assumed single reaction consuming the reactant i. The various reactions and reactants considered are detailed in the following section. The dependence of the reaction rate on the progress variables of the various species is given in a general form as $f_i(\mathbf{Y})$ as given below. Conservation of energy is expressed here as

$$\rho c_p \frac{dT}{dt} = \sum_i A_i f_i(\mathbf{Y}) \rho_i \Delta H_i \exp\left(-E_i / RT\right) + h_{eff}\left(S/V\right)\left(T_\infty - T\right) + \varepsilon\sigma\left(S/V\right)\left(T_\infty^4 - T^4\right) + Q_s \tag{2}$$

where reactions over all species i contribute according to the reaction enthalpy per unit mass for that species consumption, ΔH_i and its mass per unit volume, ρ_i. External heat flux is characterized by a heat transfer coefficient, h_{eff}, and a surface emissivity, ε, both acting over a surface-to-volume ratio, S/V. The environment temperature is T_∞.

In this work, we consider both the thermal runaway (ignition) of a single cell and the propagation from cell to cell along a pack of cells. For single cell thermal runaway a single bulk temperature within the cells is assumed to be representative leading to the relevance of Semenov's classical approach to ignition limits [1]. For propagation from cell to cell along a pack, the internal structure of the cell is homogenized, but a heat conduction term is added to Eq. (2) that describes the flux of released chemical energy to propagate the reaction front. We note that the reactants do not diffuse and the front propagation is similar to that described for reacting solids [2].

3. Chemistry and Physics of Thermal Runaway

The high energy density of lithium-ion cells brings with it high reactivity. Batteries contain internally a fuel and oxidizer, with the lithiated carbon anode acting as the fuel and a metal oxide acting as the oxidizer. The overall cell discharge is governed by the chemical reaction

$$\mathrm{C_6Li + CoO_2 \rightarrow C_6 + LiCoO_2} \quad \Delta G \approx 400 \text{ kJ mol}^{-1} \text{ Li}$$

that occurs through the mediating influence of an electrolyte composed of alky electrolytes. Under normal conditions, a passivation layer exists on the anode, referred to as the metastable SEI layer, and this decomposes at very modest temperatures (on the order of 100 C). At more elevated temperature conditions, the anode and cathode can both react with the electrolyte and

the electrolyte itself can decompose through reactions with the salt. All of these processes are overall exothermic and have been measured in calorimetry experiments of various types. Examples of reaction rates that have been extracted from these measurements are given in Table 1. Two cathode materials have been considered, one based on CoO_2 that is the most prevalent of existing cell types and another based on Mn_2O_4 that is less commercialized, but representative of a more thermally stable cathode material. While four different reaction processes are listed (with two options for cathode chemistry) in Table 1, the reaction that plays the most significant role in controlling typical ignition and propagation is the cathode-electrolyte reaction. This reaction is characterized by a sufficiently strong het release and a large activation energy that leads to rapid runaway. Reactions of the metastable SEI and the anode electrolyte can occur at lower temperatures, but are slow enough that typical heat losses can dissipate the heat release, preventing ignition by the Semonov criterion. Reactions and physical properties used for simulations are provided in Tables 1 and 2.

Table 1. Reaction rate description. For simplicity and consistency with existing literature, the reactants are expressed in normalized progress variables instead of strict mass fractions or concentrations.

Reaction description	Y_i	Initial value	$f_i(\mathbf{Y})$	A_i [s^{-1}]	E_i [kJ mol^{-1}]	ΔH_i [kJ mol^{-1}]	Ref.
Metastable SEI decomposition	Y_{SEI}	0.15	Y_{SEI}	1.7e15	135	257	[3, 4]
Anode-electrolyte reaction	Y_{C6Li}	0.45	$Y_{C6Li}\, e^{-z/0.33}$ (a)	2e13	77.2	1714	[3, 4]
Electrolyte decomposition	Y_{Elyte}	1.0	Y_{Elyte}	5.1e25	274	155	[5]
CoO_2-electrolyte reaction	Y_{CoO2}	0.96	$Y_{CoO2}(1-Y_{CoO2})$	6.7e11	122	314	[6]
Mn_2O_4-electrolyte reaction	Y_{Mn2O4}	0.96	Y_{Mn2O4}	1.1e18	218	350	[5]

(a) The source term for the anode-electrolyte is reduced by the passivation layer thickness according to $f_{C_6Li}(\mathbf{Y}) = Y_{C_6Li}\exp\left(-z/0.033\right)$ where $z = 0.033 + \left(Y_{C_6Li,0} - Y_{C_6Li}\right) + \left(Y_{SEI,0} - Y_{SEI}\right)$ is the contribution of the metastable SEI decomposition and anode-cathode reaction to this passivation layer thickness in addition to its initial thickness which is estimated at 0.033 [3, 4].

Table 2. Parameters for evolution of Eqs. (1) and (2) are representative values taken from [7].

Parameter	value	Parameter	value	Parameter	value
S/V	253 m^{-1}	λ	3.4 W m^{-1} K^{-1}	ρ_{C6Li}	363 kg m^{-3}
ρc_p	1.8e6 J m^{-3}	ε	0.8	ρ_{Elyte}	242 kg m^{-3}
h_{bl}	7.17 W m^{-2} K^{-1}	σ	5.67e-8 W m^{-2} K^{-4}	ρ_{CoO2}	726 kg m^{-3}
d	0.018 m	L	0.065 m	ρ_{Mn2O4}	1340 kg m^{-3}

4. Simulations of Thermal Runaway

In this section, we simulate thermal abuse scenarios and discuss the thermal aspects of the evolution in these cases. We discuss a single cell battery in a high temperature environment and the potential that will lead to strongly exothermic thermal runaway. All simulations are carried out using nominal properties indicated in Table 2 that are representative.

The configuration for thermal runaway (ignition) simulations is referred to as an oven test, and it simulates the response to elevated environment temperatures. These tests define a fixed environmental temperature, T_∞, with both convection and radiative heat transfer to/from a cell initially at ambient temperature as per Eq. (2). These simulations are relevant to fire environments as T_∞ can be related to the fire environment or other heat sources. Figure 1 shows the temperature evolution and its net source term at two oven temperatures for both cathode materials given in Table 1, CoO_2 and Mn_2O_4. Because of the strong activation energies associated with the various exothermic processes and especially the cathode decomposition, the environment temperature and the rate constant for the limiting reaction are the most important factors in determining the degree of thermal runaway and heating that occur. The cathode material is identified here as the limiting reaction, and two cathode materials are considered to investigate the role of material choices in thermal runaway. The cases at 150 ˚C show that the Mn_2O_4 cathode does not experience significant heat release while the CoO_2 cathode does undergo full thermal runaway.

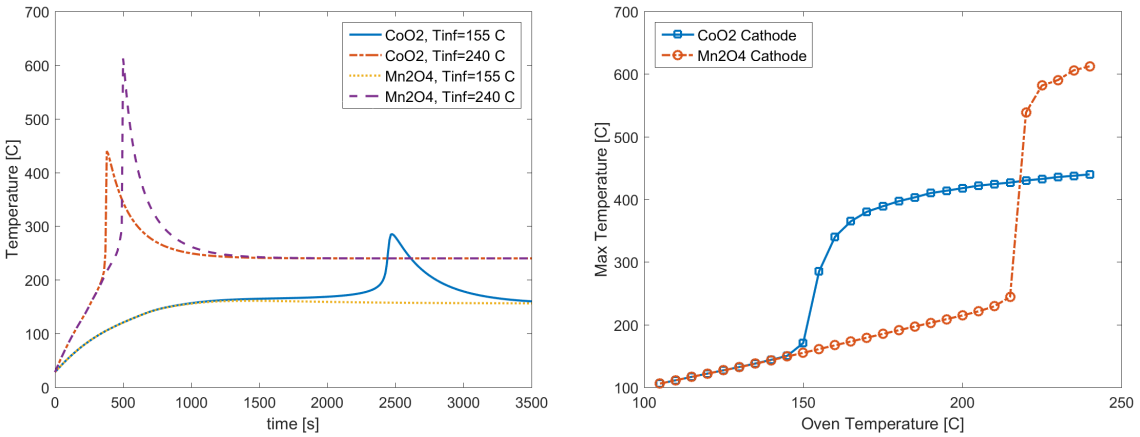

Figure 1. The temperature evolution for four cases, two temperatures with each cathode. The right panel shows the maximum temperature observed as a function of the environment (oven) temperature.

The thermal runaway temperature for each cathode material is evident in right panel of Figure 1 where the difference in the cathode chemistry leads to thermal runaway occurring around 150 ˚C and 220 ˚C for CoO_2 and Mn_2O_4 cathodes for this particular set of conditions.

For applications to vehicles and stationary energy storage, a large number of cells are assembled into battery packs. The number of cells employed can range from tens to thousands depending on the application, and a significant concern is the propagation of a cascading failure from one cell or location throughout the entire pack. Heat transfer may occur through heat conduction or through convection (the latter including electrolyte combustion external to the cell). Here we

discuss propagation due to heat conduction using a hot left boundary to initiate thermal runaway and adiabatic conditions otherwise.

It is found that the front propagates at an uneven rate as shown in Figure 2. The configuration is nominally 128 flat (pouch-type) cells stacked in a line. Here the average temperature is reported as an overall progress variable along with its rate of change. The rate of change is seen to vary by several orders of magnitude. This is reminiscent of the pulsating propagation observed in solid combustion as theoretically described in Ref. [2]. In brief, heat conduction allows heat from a reaction to propagate ahead of the reaction front while reactants are fixed (an infinite Lewis number limit). Heat propagating ahead of a reaction front leads to cooling of the reaction front and preheating of the reactants ahead. Because the rate of propagation is strongly temperature dependent, $V_{prop} \approx \sqrt{\alpha A e^{-E/RT_{peak}}}$, this local cooling of the reaction front dramatically reduces the propagation rate. When the front propagates into the preheated region in advance of the previous reaction front, the reaction temperature is increased, leading to exponentially faster propagation. This is easiest to visualize using a total enthalpy, the sum of the chemical and thermal contributions, as done in Figure 3.

It is found that the cathode reaction (CoO_2–electrolyte reaction here) is the significant process associated with the reaction front, but the heat release from the slower anode-electrolyte reaction is still important in determining the overall rate (figure not shown). In the lower left panel of Figure 2 the various reaction progress variables are shown, and it is seen there that the anode-electrolyte progress lags the reaction front when the front propagation rate is large. However, when the front propagation rate is reduced this slower anode-electrolyte reaction plays a role in supporting the overall heat release. Further work is needed to better understand this multi-stage mechanism of pulsating-front propagation for solid reacting materials.

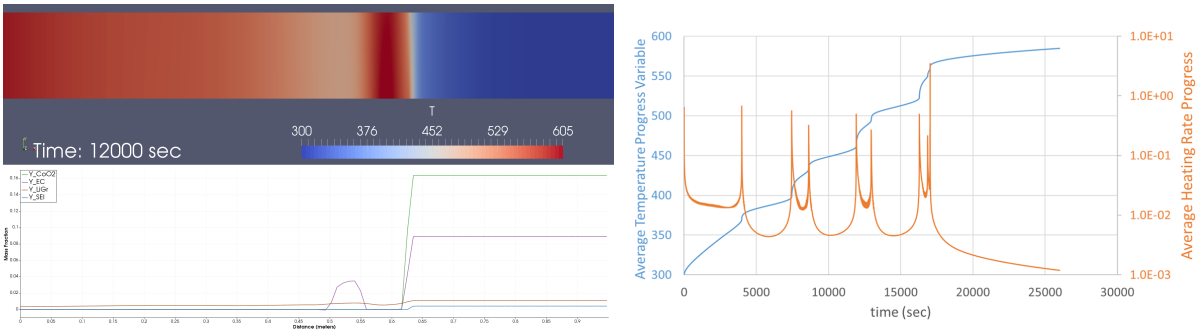

Figure 2. Propagation of the thermal front across a stack of 128 homogenized cells. The left panel shows an inhomogeneous temperature field along the length of the pack (top) and the mass fractions (bottom) each at the same instant. The right panel shows the overall progress and its rate of change in terms of an average temperature across the domain.

5. Conclusions

Predictions of thermal runaway (ignition) using calorimetry-derived reaction mechanisms are presented. These mechanisms are used to also model propagation across multiple-cell packs. Such propagation is observed to exhibit a pulsating rate, with the rate varying by several orders of magnitude. This pulsating-propagation behavior is attributed to variations in the total enthalpy asociated with heat conduction redistributing thermal enthalpy ahead of the reaction

zone, leading to fluctuations in the peak reaction zone temperature. Since propagation depends on the Arhennius rates at this peak reaction zone temperature to leading order and the activation energies are large, these fluctuations in the total enthalpy are signficant.

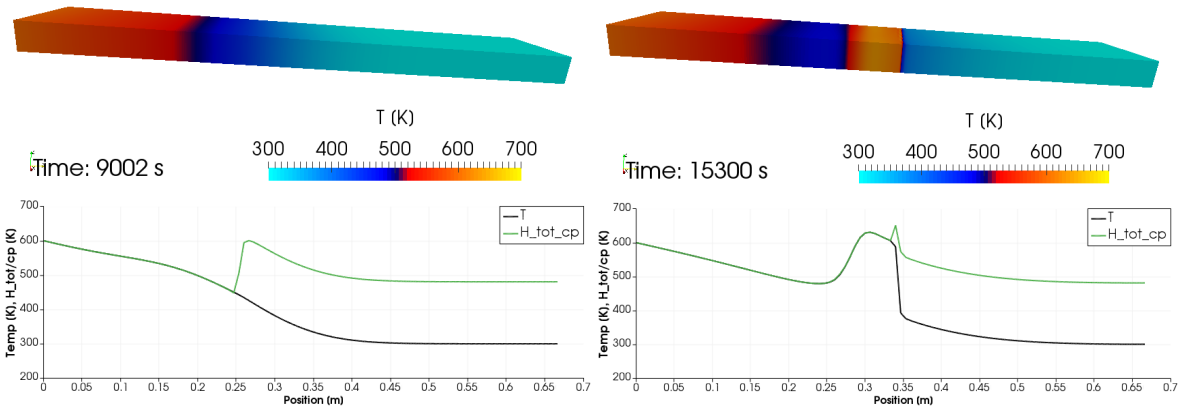

Figure 3. Reaction front propagation with simplified chemistry (cathode reaction only but with twice the nominal heat release). In the left panel the reaction front is propagating through a region where heat conduction has reduced the total enthalpy by transferring reaction het in advance of the front, leading to a reduced reaction rate that also enhances the imbalance between conduction and propagation. In the right panel, the reaction front has moved into the region of higher total enthalpy, the peak temperature is greater and the front propagation is fast relative to conduction (leading to steep temperature gradients).

6. Acknowledgements

Sandia National Laboratories is a multi-program laboratory operated by Sandia Corporation, a Lockheed Martin Company for the United States Department of Energy's National Nuclear Security Administration under contract DE-AC04-94AL85000. The authors gratefully acknowledge funding from the Department of Energy, Office of Electricity's Energy Storage Program. The authors would like to thank Dr. Imre Gyuk for his support and guidance of this effort.

6. References

1. Frank-Kamenetskii, D.A., *Diffusion and Heat Exchange in Chemical Kinetics, 2nd ed.* 1969: Plenum.
2. Matkowsky, B.J. and G.I. Sivashinsky, *Propagation of a pulsating reaction front in solid fuel combustion.* SIAM J. Appl. Math., 1978. **35**(3): p. 465-478.
3. Richard, M.N. and J.R. Dahn, *Accelerating rate calorimetry study on the thermal stability of lithium intercalated graphite in electrolyte I. Experimental.* J. Electrochem. Soc., 1999. **146**(6): p. 2068-2077.
4. Richard, M.N. and J.R. Dahn, *Accelerating rate calorimetry study on the thermal stability of lithium intercalated graphite in electrolyte II. Modeling the results and predicting differential scanning calorimeter curves.* J. Electrochem. Soc., 1999. **146**(6): p. 2078-2084.
5. Spotnitz, R. and J. Franklin, *Abuse behavior of high-power, lithium-ion cells.* J. Power Sources, 2003. **113**(1): p. 81-100.
6. MacNeil, D.D., et al., *An autocatalytic mechanism for the reaction of LixCoO2 in electrolyte at elevated temperature.* J. Electrochem. Soc., 2000. **147**(3): p. 970-979.
7. Hatchard, T.D., et al., *Thermal model of cylindrical and prismatic lithium-ion cells.* J. Electrochem. Soc., 2001. **148**(7): p. A755-A761.